

An Study on Medical imaging and radiation therapy treatment technologies

Atul Bisht

Asst. Professor, Department of Physics, Graphic Era Hill University, Dehradun, Uttarakhand India
248002,

Abstract:

Cancer patients still benefit greatly from radiation treatment (RT). There has been a lot of focus recently on incorporating MRI into the implementation and assessment of RT in clinical settings. MRI has been included into RT under the designation MRI-guided RT because to its superiority over CT in the monitoring of tumor and tissues physiologic changes, the imaging of soft tissues, and the imaging of organ movements. Offline magnetic resonance imaging (MRI) is already being used by several hospitals for healthcare planning. In addition, MRI-guided linear acceleration systems allow for a more rapid reaction to alterations in anatomy between RT fractions, making them preferable to CT guidance. Tumors affected by mobility are now undergoing MRI-guided intrafraction adaptive RT, and biomarkers derived from MRI are being developed to assess treatment response and perhaps modify therapy to physiological changes. These MRI-guided advancements provide the groundwork for a paradigm change in the design, monitoring, and adjustment of therapy. Methods for "real-volumetric anatomic imaging," correction of image distortion caused by electromagnetic field inhomogeneities, reproducible quantitative imaging across a variety of MRI infrastructure, and biological validation of quantitative imaging are all crucial steps toward improved MRI-guided RT. New developments in both online and offline MRI-guided RT are discussed, along with their potential for improving research and therapeutic treatment, challenges they present, and the need of interdisciplinary cooperation in overcoming these concerns..

Keywords: imaging biomarker, microenvironment, MRI, quantitative imaging, radiation

Introduction

When it comes to traditional cancer treatment methods like surgery, chemotherapy, immunotherapy, etc., radiation therapy (RT) is by far the most often used therapeutic technique.^{1,2} However, RT causes multi-organ malfunction and mortality due to collateral damage to normal tissues and organs.^{3,4} High mortality rates and limited treatment options characterize patients with advanced malignancies such glioblastoma multiforme, pancreatic, and lung cancers.⁵ Improvements in local tumor management and higher survival times have resulted from recent technological developments in RT.^{5–7} Depending on the treatment area, radiation treatment (RT) may be classified as external beam radiation therapy (EBRT), internal beam radiation therapy (IBRT), brachytherapy, or systemic radioisotope therapy (SRT). Image-guided radiation has replaced traditional radiotherapy as the preferred method of treatment for the vast majority of diagnoses and treatments since 2005, when on-board cone-beam computerized tomography (CBCT) equipment became generally available. Patients have had better tumor control and fewer negative side effects as a consequence [1]. Since then, advancements in imaging have likely contributed to a number of paradigm shifts [2,3] in the field of

radiation. However, technologies like linear accelerators that integrate with on-board MR imaging and the possible future of MR-guided particle therapy [4,5] are being explored in clinic to improve accuracy and precision of delivery. This article compares and contrasts the voxelization, adaptability, and our own "response" hypotheses. Their development relies heavily on the underexplored but potentially game-changing physiological and metabolic imaging elements [6]. Voxel-by-voxel analysis of the tumor microenvironment was made possible with their help. More precise assessments of therapy response and modifications to the tumor microenvironment would be possible, as would the use of techniques like dosage mapping in radiation planning. Early detection and effective treatment are cornerstones of individualized cancer care. CT and MRI, with or without contrast-enhancing tracers, are examples of "direct" signal questioning of tumor physiology; "indirect" approaches, whereby the detected signal is a by-product of cancer metabolism and is typically measured with PET or positron emission tomography after glucose or oxygen consumption, are frequently referred to as "metabolic" imaging. This article focuses on the use of functional imaging in the treatment of primary tumors and metastases in the brain using stereotactic radiation and (systemic) immunotherapy. In order to ascertain whether or not functional parametric pictures can be generated, how effectively they define the microenvironment of tumors, and whether or not they can be relied upon for use in treatment planning and outcome evaluation, the outcomes of phase I and II clinical trials shall be reviewed. Let's start by looking at the idea of a valid clinical objective closely. The use of flow imaging and metabolic MRI/PET in the study of biological phenomena is expected to increase in the near future. In place of a comprehensive systematic literature evaluation, we will focus on works that lend credence to the hypotheses and possibly paradigm-shifting procedures of a biology-tailored approach to cancer therapy. Potential advantages of computer image processing technology and artificial intelligence will be explored, as will the dependability of applying multiparametric techniques in normal radiation oncology treatments. It is now understood that the tumor microenvironment plays a role in the reprogramming of metabolism in brain tumors, which in turn causes decreased treatment sensitivity or tumor recurrence. Metabolic anomalies in primary brain tumors may be used for noninvasive tumor scanning, offering up fresh therapeutic options for better diagnosis and assessment of therapy efficacy.

External Beam Radiation Therapy (EBRT)

Doctors use external beam radiation therapy (EBRT) to treat advanced localized cancer. Cancer cells die or cannot multiply after DNA damage, cell cycle arrest, cytogenetic damage, and senescence.⁶ When used to treat cancer, radiation damages both healthy and cancerous cells.¹⁰ Cancer cells die while healthy ones survive. Photon radiation (X-rays and gamma rays) and electron beams are used to treat tumors near the skin. Proton and neutron beams are efficient against metastatic malignancies in deep organs and tissues. Particle beam radiation treatment may now evenly dose deep-seated tumors. Radiation's RBE quantifies cell death. Radiotherapy effectiveness depends on tissue and cell response, splitting rate, overall dosage, and LET. X-rays and gamma rays convey little energy. Higher LET (neutrons and protons) radiation deposits more energy at target areas. Radiation excites cell water molecules, causing secondary DNA damage.¹² Cell death is caused by double-strand DNA breaks in healthy and malignant tissues. Single-strand DNA breakage seldom kills cells. Radiation treatment stops and kills cancer cells. Cancer cells cease proliferating and die when DNA is irreparably broken. Understanding radiation-induced cell death pathways may enhance radiation treatment. EBRT can be intensity-modulated, stereotactic, image-guided, three-dimensional modulated arc, proton, or heavy ion beam therapy, depending on the tumor type and disease dynamics. Computer scanning and assessment algorithms, dose computation infrastructure, and delivery methods have improved tumor dose distribution, delineation, and normal tissue irradiation. This paper discusses the many technical advances in EBRT methods and their pros and cons to improve cancer treatment..

Dimensional Conformal Radiotherapy (3DCRT)

3D conformal radiation (3DCRT) is EBRT that requires 3D treatment planning, numerous cross-firings, and well-built fixed fields.¹³ 3DCRT uses CT imaging instead of X-rays to better arrange and shield beams. 3D conformal radiation is being used for brain, breast, gastrointestinal, lung, and genitourinary cancers. 3D conformal radiation (3DCRT) and intensity-modulated radiotherapy (IMRT) reduce short-term response rate, mouth dryness, and parotid gland damage in nasopharyngeal cancer patients, improving their future and quality of life.¹⁴ 3DCRT-treated endometrial cancer patients had more gastrointestinal damage than IMRT patients.¹⁵ 3DCRT makes placement, scans, contouring, dosimetry, tracking, and dosing complex..

Literature Review

Martina De Landro et.al.,(2020) MRT-directed laser interstitial thermal treatment (LITT) is showing promising outcomes in many organs, including the brain. Think about changing the MRT's protons resonance frequency (PRF) for tissue independence. PRF shift-based MRT has issues that lower temperature map confidence despite its promise. MRT-guided LITT temperature maps are inaccurate because to susceptible gas bubble formation errors. MRT-guided LITT susceptibility artifacts are characterized and sized. A 1.5 T clinical MRI scanner conducted LITT on gelatin phantoms at 5 W, 2 W, 1 W, and 0.5 W. 3D Echo-planar imaging prototypes obtained the temperature pictures. Erroneous zones with -2°C or higher temperature variations. The artifact's sagittal, axial, and coronal shapes were also examined. The vulnerability of the artifact is a double lobe and most broadly distributed in the sagittal plane, according to study. The stronger laser may have caused the larger artifact region. Avoiding susceptibility artifacts during MRT-guided LITT was shown using 80°C temperature deviations. The examination of the laser's power on the artifact reveals that a low-powered laser (0.5 W) may reduce this measurement inaccuracy.

Hongyi Duanmu et.al.,(2020) Radiation dosage prediction and plan optimization employ 3D organ contouring. Manual contouring takes time and may dilute research results by adding clinic variance. These organs range from a few hundred milliliters to several thousand. This paper introduces BrainSegNet, a 3D fully convolutional neural networks (FCNN)-based autonomous brain organ segmentation method. Brain-SegNet uses various resolution paths and a weighted loss function to address organ sizes. We tested our technique using 46 Brain CT image volumes annotated with expert organ outlines. BrainSegNet beats LiviaNet and V-Net on narrow organs like the chiasm, optic nerves, and cochlea. BrainSegNet may increase radiation treatment efficiency by decreasing physical contouring from an hour to two minutes.

Methodology

We employ the Hamiltonian Engine for Radiotherapy Optimization (HERO) to design IMRT treatments in this study. HERO splits and approximates large generalform binary optimization problems using a quadratic pseudo-boolean function. When optimizing the function, quadratic unconstrained binary optimization (QUBO) commonly arises. IMRT optimization and other QUBO issues have been studied using quantum annealing (QA). The QA can only handle a limited number of variables, and achieving optimal designs takes hours. HERO, an optimizer for QUBO problems, overcomes these limits and works normally at ambient temperature with ordinary hardware. Seven prostate IMRT instances with an average of 6,000 beamlets are used to assess HERO. Our method's speed and quality were compared to Eclipse, a commercial treatment planning program. HERO solves tasks in 30 seconds, but Eclipse may take several minutes. HERO may help optimize radiation

treatment, according to the studies. With HERO, complex treatments like Volumetric Modulated Arc Therapy (VMAT) may be designed..

Volumetric Modulated Arc Therapy (VMAT)

By accurately adjusting the dosage-rate and multileaf collimator (MLC), VMAT can deliver the whole dose volume in one revolution in any of the 360 degrees. The MLC needs controls because adding monitor units (MU) and beam orientations slows therapy. Because the tumor rotates, various regions get different doses. VMAT spares organs better than IMRT because it doses surrounding tissue less. VMAT uses less MU than IMRT, reducing the incidence of second malignancies. However, low-dose washing away too much normal tissue may counterbalance the risk reduction. In painful immobilization cases such as head and neck malignancies, VMAT therapy reduces OAR irradiation and has higher uniformity than IMRT. VMAT with the simultaneous integrated boost (SIB) method improves local tumor control, survival, and tolerability in advanced non-small cell lung cancer (NSCLC) patients who are not candidates for traditional final therapy.²¹ VMAT has been utilized in planning and clinical outcome studies for prostate, gastrointestinal, gynecological, head and neck, thoracic, nervous system, and breast cancers.²² VMAT may increase the likelihood of second cancers by exposing more organs and tissue to low-dose radiation. Thus, to assess secondary cancer risk, patients should be monitored for longer..

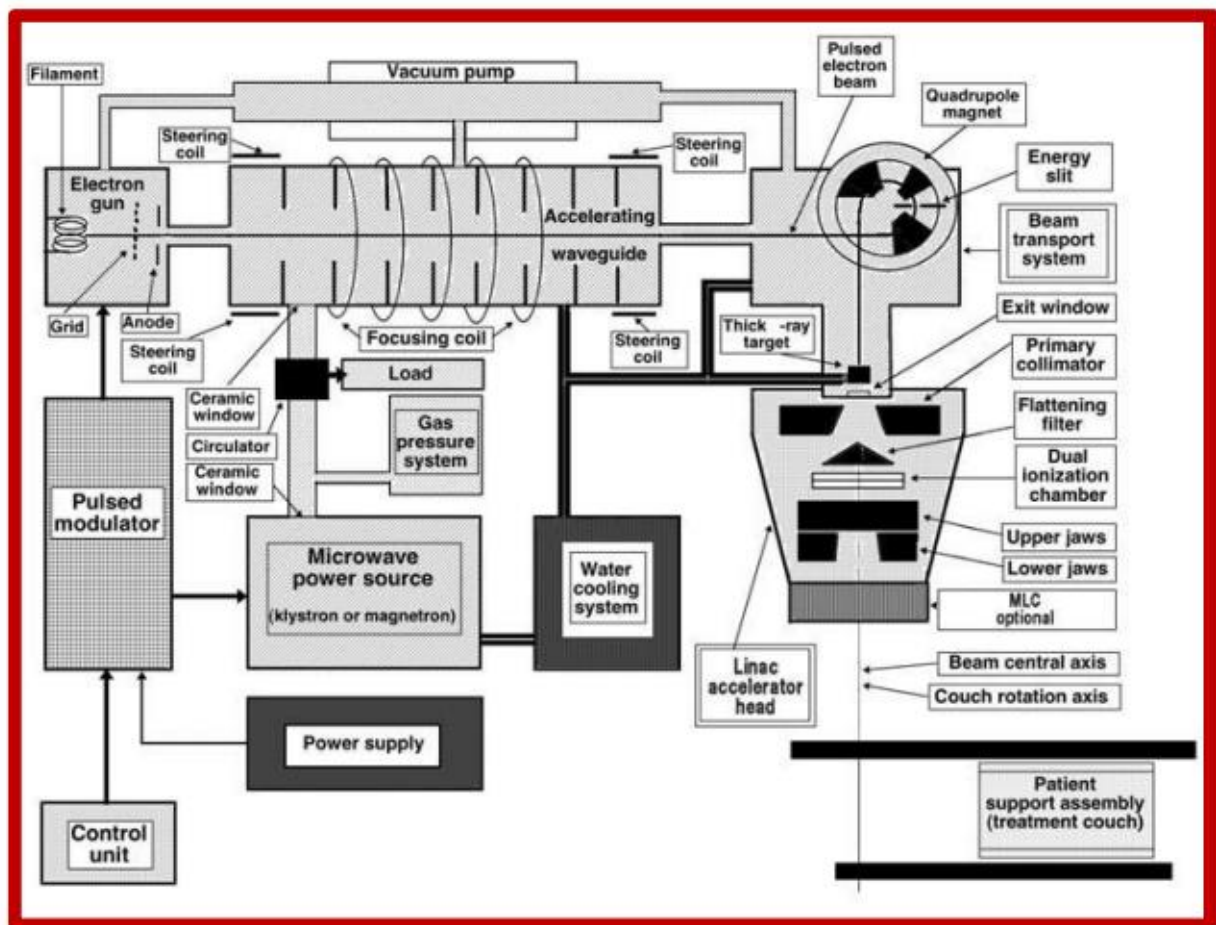


Figure 1: Schematic Diagram of a Medical linear accelerator with its components

A microwave generator with a modest output will provide the necessary energy. For beam energies over 20 MeV, klystrons are preferred over magnetrons due to their longer endurance and higher power generation. Linacs producing energies of up to 6 MeV use very short accelerator tubes. To deflect electrons 90 (or 270) degrees, higher energy Linacs often position a longer accelerator tube perpendicular to the treatment head axis and use bending magnets. The last part of a Linac is the treatment head. Target, collimator, scatter foil, monitor ionization chambers, flattening filters, and maybe other beam changing devices are only some of the parts that make up this apparatus. Modern linear accelerators may be used for both x-ray and electron therapy. Bremsstrahlung beams of photons are produced when fast-moving electrons hit a high-atomic-number target.

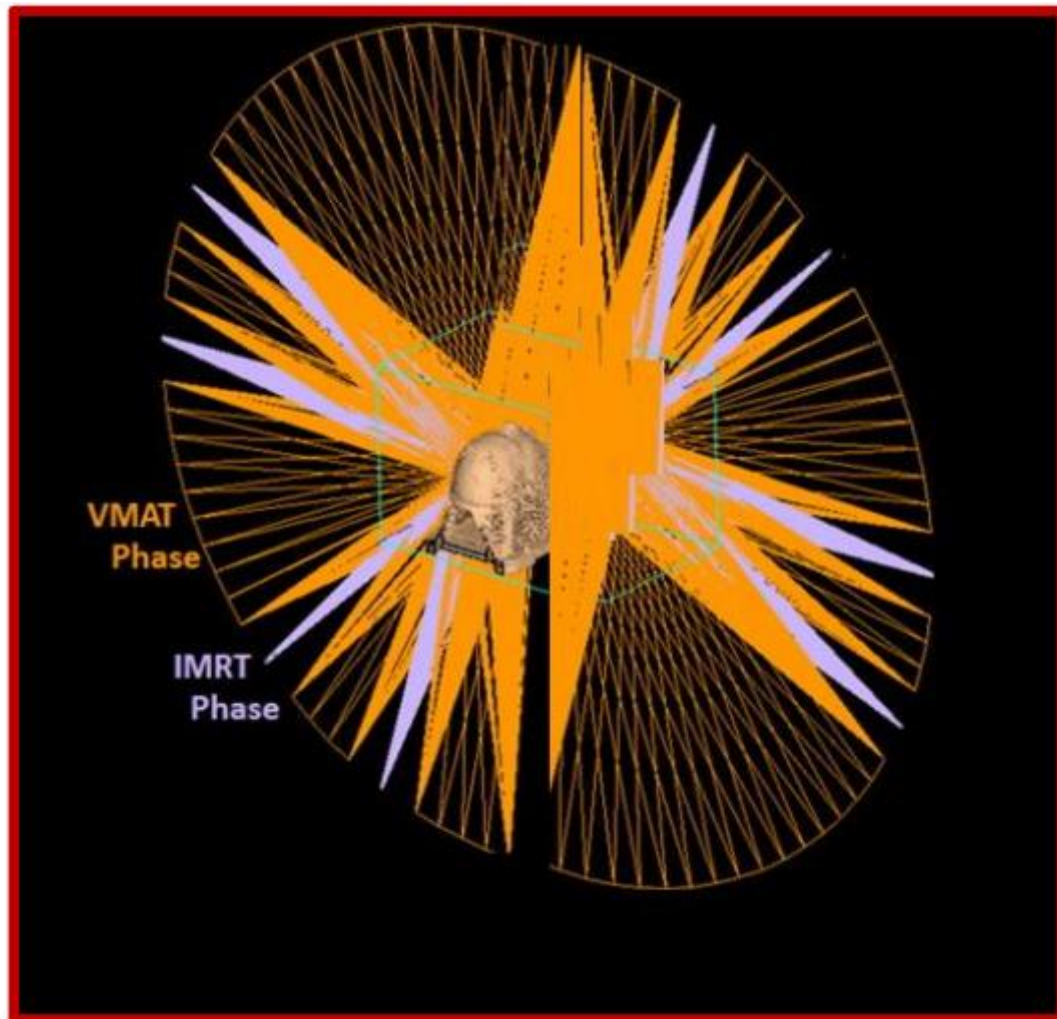


Figure 2: The Single Image Representing comparison of IMRT and VMAT planning and delivery

With VMAT technology, the target is continuously irradiated as the beam source revolves in a single or several arcs around the patient (11). By concurrently adjusting the gantry speed, gantry location, collimator angle, leaves of the MLC, and dose rate, as illustrated in figure 2, a high degree of conformal dose coverage may be obtained in a much shorter amount of time than with existing approaches. VMAT sessions typically last 5 minutes or less [12], and use 3D imagery of the actual patient to confirm the target's location.

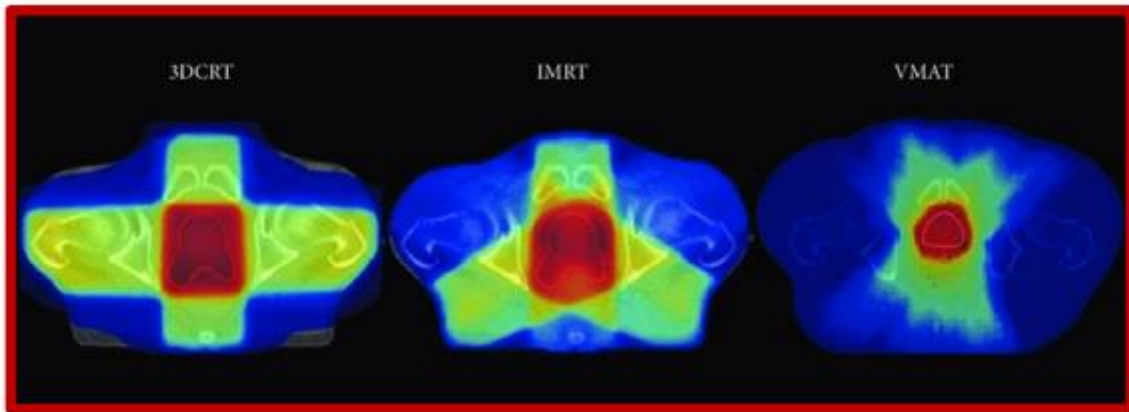


Figure 3: The isodose distribution generated from 3DCRT, IMRT AND VMAT Planning with 6 MV Photon energy



Figure 4: Two partial co-planar arcs and volumetric modulated arc treatment are used in SRS treatment for a patient with left cerebellar metastases (VMAT).

One session of SRS may be sufficient to treat the whole spine and brain. Body radiosurgery is used to treat cancers of the lungs, liver, adrenal glands, and other soft tissues, and it often consists of many (three to five) treatment sessions.

The following calculating characteristics were considered while making the VMAT plans: The Monte Carlo variation was set at 3%, and the grid spacing was set at 3 mm. For the second and final step of dosage calculation, the Monte Carlo method was used as the secondary algorithm. The medium, not the water, was used in the dosage calculation. Heterogeneity correction was performed on all of the plans. The whole VMAT plan was supplied in one continuous arc of gantry rotation (from 180 degrees clockwise to 180 degrees counterclockwise). For the purpose of MLC segmentation in the VMAT method, the sweep sequencer tool was used. In VMAT plan, the photon field strength is varied along a gantry arc, as opposed to being constant in IMRT. Using the 'IGA' option, the proposed VMAT arc was partitioned into equal-sized sectors (Figure 1). During continuous irradiation, MLC segments shifted from right to left inside a sector and then back again within the next sector, allowing for intensity modulation. This resulted in a back-and-forth pattern of intensity modulations between succeeding sections. The recommended dosage was administered through VMAT using a photon beam that had been flattened to 6 MV. Optimized VMAT plans (VMAT,10, VMAT,20, VMAT,30, and VMAT,40) were generated by changing the value of the parameter 'IGA' (from 10 degrees to 20 degrees to 30 degrees to 40 degrees).

Using optimization parameters (Table 2) and computation parameters (Table 3), VMAT plans were optimized to meet the requisite dosage restrictions (Table 1). On 3D CT scans, we determined the radiation dosage from the VMAT plan and made use of heterogeneous adjustments..

Structure	Parameter	Constraints
PTV	$V_{95\%}$	$> 47.5\text{Gy}$
	$V_{10\%}$	$< 107\%$ of Prescribed Dose
Rectum	$V_{60\%}$	$< 45\text{ Gy}$
Bladder	$V_{35\%}$	$< 45\text{ Gy}$
Bowel	D_{Max}	$< 50\text{ Gy}$
Femoral Head	$V_{20\%}$	$< 40\text{ Gy}$

Table 1. Treatment planning objectives for VMAT

Structure	Cost functions	Parameter	Isoconstraints
PTV	Target EUD	0.5	50 Gy
	Quadratic Overdose	51.5 Gy	0.45Gy
	Target penalty	95%	50 Gy
Rectum	Parallel	k=3	35 Gy
Bladder	Parallel	k=3	30 Gy
Bowel	Parallel	k=3	25 Gy
	Maximum dose	Shrink=3 mm	48 Gy
Femoral Head	Maximum dose	Shrink=3 mm	48 Gy
Body	Quadratic Overdose	Shrink=0 mm, 50 Gy	0.10 Gy
	Quadratic Overdose	Shrink=3 mm, 47 Gy	0.15 Gy
	Maximum dose	Shrink=5 mm	46 Gy
	Maximum dose	Shrink=10 mm	40 Gy
	Maximum dose	Shrink=15 mm	35 Gy
	Maximum dose	Shrink=25 mm	25 Gy

EUD-Equivalent Uniform Dose; k=Power law exponent

Table 2. The cost functions for optimization of VMAT plans in cervical cancer

Sequencing Parameters	
Max number of Arcs	1
Max. control points per Arc	200
Min. Segment Width	0.5 cm
Fluence Smoothing	Medium
Calculations Properties	
Grid Spacing	0.3 cm
Dose Deposition to	Medium
Algorithm	Monte Carlo photon
Statistical Uncertainty	1% / calculation

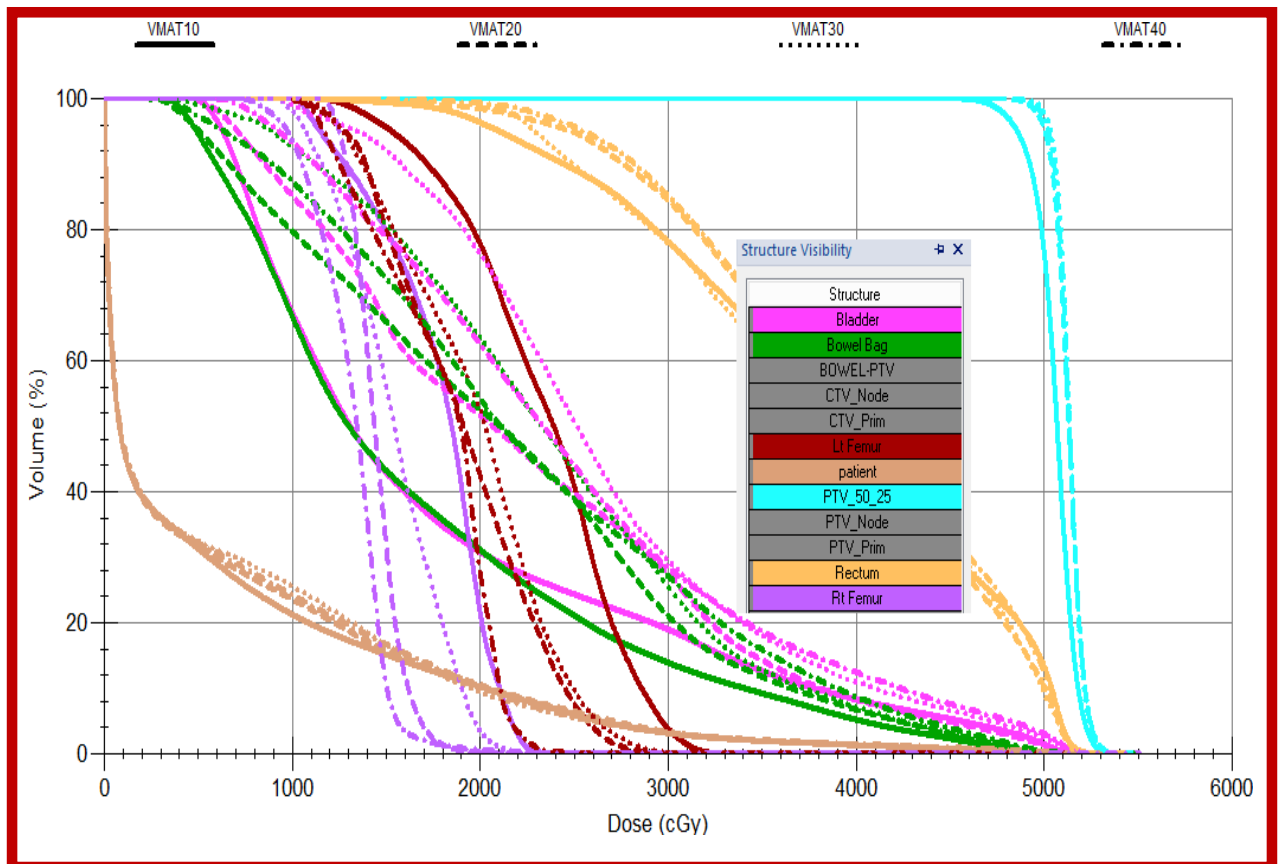
Table 3. Sequencing parameters and calculation properties for VMAT plans

Figure.4 DVH comparison for target coverage and OARs for range of IGAs VMAT plans.

Conclusion:

We included 27 patients, all of whom had carcinoma of the cervix, in our trials. Their ages ranged from 54 to 69. The cervical carcinoma in all the participants in this research was at the T3N1M0 stage. [16] They were all getting ready to undergo final radiation treatment for lymph nodes that had developed. The whole VMAT plan was supplied in one continuous arc of gantry rotation (from 180 degrees clockwise to 180 degrees counterclockwise). For the purpose of MLC segmentation in the VMAT method, the sweep sequencer tool was used. The recommended dosage was administered through VMAT using a photon beam that had been flattened to 6 MV. We optimized four different VMAT plans by changing the value of the parameter 'IGA' (to 10, 30, and 40 degrees, respectively), and we've given them the corresponding names. Better plan quality indices cannot be attained without first specifying the angular space/increment size in the VMAT method. This research shows that VMAT30 and VMAT40 may improve plan quality indexes and therapeutic gain. This research suggests that for a patient with cervical cancer, the bigger IGA (30°) may be more effective when the number of sectors is even.

References

1. M. J. Cameron *et al.*, "Characterization of 3-D-Mesa Silicon Single Strip Detectors for Use in Synchrotron Microbeam Radiation Therapy," in *IEEE Transactions on Radiation and Plasma Medical Sciences*, vol. 4, no. 4, pp. 470-478, July 2020, doi: 10.1109/TRPMS.2019.2948466.
2. H. Duanmu *et al.*, "Automatic Brain Organ Segmentation with 3D Fully Convolutional Neural Network for Radiation Therapy Treatment Planning," *2020 IEEE 17th International Symposium on Biomedical Imaging (ISBI)*, Iowa City, IA, USA, 2020, pp. 758-762, doi: 10.1109/ISBI45749.2020.9098485.
3. P. Palaniappan *et al.*, "A 2D-3D Deformable Image Registration Framework for Proton Radiographies in Adaptive Radiation Therapy," *2019 IEEE Nuclear Science Symposium and Medical Imaging Conference (NSS/MIC)*, Manchester, UK, 2019, pp. 1-3, doi: 10.1109/NSS/MIC42101.2019.9059647.
4. S. Kiml *et al.*, "Operation of Compact X-Band Linear Accelerator System Mounted on the Gantry for Radiation Therapy," *2019 International Vacuum Electronics Conference (IVEC)*, Busan, Korea (South), 2019, pp. 1-2, doi: 10.1109/IVEC.2019.8745182.
5. T. Aso, H. Oke and T. Nishio, "Range Verification using Prompt Gamma-rays with Energy Spectral Analysis in Geant4 Based Proton Therapy Simulation," *2019 IEEE Nuclear Science Symposium and Medical Imaging Conference (NSS/MIC)*, Manchester, UK, 2019, pp. 1-5, doi: 10.1109/NSS/MIC42101.2019.9059688.
6. X. Bao, W. Gao, D. Xiao, J. Wang and F. Jia, "Bayesian model-based liver respiration motion prediction and evaluation using single-cycle and double-cycle 4D CT images," *2019 International Conference on Medical Imaging Physics and Engineering (ICMIPE)*, Shenzhen, China, 2019, pp. 1-6, doi: 10.1109/ICMIPE47306.2019.9098228.
7. H. Xu *et al.*, "Radiomics-based prediction of symptomatic intracerebral hemorrhage before thrombolysis therapy in unenhanced CT imaging," *2018 IEEE Nuclear Science Symposium and Medical Imaging Conference Proceedings (NSS/MIC)*, Sydney, NSW, Australia, 2018, pp. 1-4, doi: 10.1109/NSSMIC.2018.8824456.
8. H. Zhang *et al.*, "Detector Development for Prompt Gamma Imaging in Proton Therapy Online Monitoring," *2018 IEEE Nuclear Science Symposium and Medical Imaging Conference Proceedings (NSS/MIC)*, Sydney, NSW, Australia, 2018, pp. 1-5, doi: 10.1109/NSSMIC.2018.8824761.
9. J. Vrba, J. Vrba, D. Vrba, O. Fišer and I. Merunka, "Microwaves in Medical Diagnostics and Treatment," *2018 Progress in Electromagnetics Research Symposium (PIERS-Toyama)*, Toyama, Japan, 2018, pp. 155-159, doi: 10.23919/PIERS.2018.8597911.
10. M. Povoli *et al.*, "Functional characterisation of novel silicon beam monitors for the micro-beam radiation therapy," *2015 IEEE Nuclear Science Symposium and Medical Imaging Conference (NSS/MIC)*, San Diego, CA, USA, 2015, pp. 1-4, doi: 10.1109/NSSMIC.2015.7581894.
11. Y. Nikawa and S. Nakamura, "Microwave application in medical sensing," *2015 9th International Symposium on Medical Information and Communication Technology (ISMICT)*, Kamakura, Japan, 2015, pp. 131-133, doi: 10.1109/ISMICT.2015.7107513.
12. L. Yu, X. Hui-Jun, Z. Su-Jing and Y. Xiao, "Detection and Evaluation on the Spine Tracking Accuracy during Image-Guided Radiation Therapy," *2015 Seventh International Conference on Measuring Technology and Mechatronics Automation*, Nanchang, China, 2015, pp. 374-376, doi: 10.1109/ICMTMA.2015.96.